Practical limitations of near-field goniophotometer measurements imposed by a dynamic range mismatch

Jan Audenaert, Paula C. Acuña R., Peter Hanselaer, and Frédéric B. Leloup*

Light and Lighting Laboratory, Department of Electrical Engineering (ESAT-ELECTA), KU Leuven, Gebroeders De Smetstraat 1, 9000 Gent, Belgium

**Frederic.Leloup@kuleuven.be*

Abstract: Within near-field goniophotometry, measurement results of both an imaging luminance measurement device and a photometer detector are combined to generate the luminous intensity distribution of a light source. The simultaneous use of these two detectors may engender incorrect measurement results, due to their difference in dynamic range. In this paper, near-field and far-field based luminous intensity distribution measurements of two luminaires are presented, in order to exemplify the problem. Results demonstrate that the distributions obtained from near-field measurements may deviate from the correct intensity distribution, by an amount of up to 16% of the total luminous flux of the luminaire. A method to check for the correctness of the luminous intensity distribution from the near-field measurement, the so-called sanity check, is discussed. To conclude, some possible solutions to eliminate the dynamic range mismatch induced errors are treated.

OCIS codes: (120.0120) Instrumentation, measurement, and metrology; (120.5240) Photometry.

References and links

1. J. W. T. Walsh, *Photometry* (Constable and Company Ltd, 1926).
2. S. Stannard and J. Brass, "Application distance photometry," J. Illum. Eng. Soc. **19**(1), 39–46 (1990).
3. R. Poschmann, M. Riemann, and F. Schmidt, "Verfahren und anordnung zur messung der lichtstärkeverteilung von leuchten und lampen," Patent DE 41 10 574 v. 30.3.1991.
4. P. Y. Ngai, "On near-field photometry," J. Illum. Eng. Soc. **16**(2), 129–136 (1987).
5. I. Ashdown, "Near-field photometry: a new approach," J. Illum. Eng. Soc. **22**(1), 163–180 (1993).
6. I. Ashdown and M. Salsbury, "A near-field goniospectroradiometer for LED measurements," Proc. SPIE **6342**, 634215 (2007).
7. M. López, K. Bredemeier, N. Rohrbeck, C. Veron, F. Schmidt, and A. Sperling, "LED near-field goniophotometer at PTB," Metrologia **49**(2), S141–S145 (2012).
8. M. Lopez, K. Bredemeier, F. Schmidt, and A. Sperling, "Near-field goniophotometry: a metrological challenge," in *Proceedings of the Simposio de Metrologia, Santiago de Querétaro* (CENAM, 2010).
9. F. Schmähling, G. Wübbeler, M. Lopez, F. Gassmann, U. Krüger, F. Schmidt, A. Sperling, and C. Elster, "Virtual experiment for near-field goniophotometric measurements," Appl. Opt. **53**(7), 1481–1487 (2014).
10. J. Audenaert, G. Durinck, F. B. Leloup, G. Deconinck, and P. Hanselaer, "Simulating the spatial luminance distribution of planar light sources by sampling of ray files," Opt. Express **21**(20), 24099–24111 (2013).
11. J. Audenaert, F. B. Leloup, B. Van Giel, G. Durinck, G. Deconinck, and P. Hanselaer, "Impact of the accurateness of bidirectional reflectance distribution function data on the intensity and luminance distributions of a light-emitting diode mixing chamber as obtained by simulations," Opt. Eng. **52**(9), 095101 (2013).
12. V. Jacobs, S. Forment, P. Rombauts, and P. Hanselaer, "Near-field and far-field goniophotometry of narrow-beam LED arrays," Lighting Res. Technol. doi:1477153514530139 (2014).
13. H. Technoteam Bildverarbeitung Gmb, *http://www.technoteam.de/produktuebersicht/rigo801/produkte/index_ger.html*
14. *Modular Lighting Instruments,* http://www.supermodular.com
15. I. Ashdown, "Comparing photometric distributions," in *Proceedings of the11th Canadian Conference on Computational Geometry* (CCCG, 2000).
16. A. S. J. Bergen, "A practical method for comparing luminous intensity distributions," Lighting Res. Tech. **44**(1), 27–36 (2012).

#221751 - $15.00 USD Received 26 Aug 2014; revised 10 Dec 2014; accepted 21 Jan 2015; published 28 Jan 2015

17. K. Bredemeier, R. Poschmann, and F. Schmidt, "Development of luminous objects with measured ray data," Laser Photonik **2**, 20–24 (2007).
18. I. Ashdown, "Near-field photometry in practice," in *IESNA Annual Conference Technical Papers* (Illuminating Engineering Society of North America, 1993), pp. 413–425.

1. Introduction

The far-field intensity distribution of a light source or luminaire, better known as the luminous intensity distribution (LID), is one of the key characteristics of a lighting device which is used to perform lighting calculations and simulations. The determination of the LID is conventionally performed by use of a far-field goniophotometer, by which the illuminance is recorded at various angles around the device under test (DUT). The distance between the detector and the DUT is thereby kept invariant and larger than the limiting photometric distance, such that the DUT can be assumed to be a point source [1, 2]. By application of two fundamental photometric laws, known as the inverse square law and the cosine law [1], the LID can then be determined from the illuminance data.

Since the beginning of the 1990s, near-field goniophotometry (NFG) has been introduced as an alternative method to measure the LID [3–5]. While far-field goniophotometry (FFG) relies on illuminance data captured by a photometer, NFG starts from the luminance distribution acquired by use of an imaging luminance measurement device (ILMD) [6, 7]. To this end, the ILMD revolves about the DUT, and captures luminance images for all directions in which light is emitted. No restrictions are thereby imposed on the distance between the ILMD and the DUT, such that generally this distance is smaller than the limiting photometric distance, i.e., within the near-field. Each pixel p in the luminance images defines a solid angle element $d\Omega_p$ and an area element dA_p, and ultimately, a discrete luminous flux portion $d\phi_p$ (for a full description of the measurement principle, see [7]). The final set of luminous flux portions from all pixels at all camera positions yields a ray file, i.e., a list of rays characterized by a starting point, a direction of propagation, and a luminous flux. From this ray file, far-field quantities such as the LID and the total luminous flux can be derived.

Compared to FFG, NFG offers some important advantages [8, 9]. From a practical point of view, near-field measurements can be made with smaller and cheaper equipment [9]. Furthermore, the ray files of light sources can be used in ray tracing software for the design of new luminaires, by simulating the interactions with other optical components (reflectors, filters, etc.) [10, 11]. As such, NFG enables the simultaneous determination of both near-field related characteristics, such as the near-field illuminance [12] and the luminance distribution from the luminaire, as well as far-field related quantities, i.e., the LID and the total luminous flux.

Practical near-field goniophotometers are generally equipped with at least two detectors. Besides the ILMD, also a photometer revolves about the DUT. The ILMD is thereby used to capture the luminance distributions, while the photometer provides illuminance values. The luminance distributions, measured at each position, are then weighted with the total luminous flux, obtained by integration of all illuminance values. The main reason for still using a photometer detector is that the uncertainty on the reported flux from the photometer measurements is lower than the uncertainty on the flux calculated from the ILMD measurements. From a practical point of view, the photometer can furthermore be used as a single detector if only the far-field characteristics are requested, supposing that the dimensions of the DUT are small enough compared to the distance between the DUT and the photometer. Indeed, the near-field goniophotometer can then be used to measure under far-field conditions with only the photometer, speeding up the acquisition.

Yet, the simultaneous use of an ILMD and a photometer under near-field conditions may engender incorrect measurement results. Typically, these detectors exhibit a different dynamic range, the dynamic range of the ILMD being inferior to that of the photometer. Two issues may result from this dynamic range mismatch. First, within certain directions, the ILMD may not capture the luminance distribution because of a too low signal, while the

#221751 - $15.00 USD Received 26 Aug 2014; revised 10 Dec 2014; accepted 21 Jan 2015; published 28 Jan 2015

photometer detects an emitted flux. Second, luminance values below the detection limit of the ILMD may not be incorporated within a relative luminance distribution image.

In this paper, near-field and far-field based LID measurements of two luminaires are presented, in order to exemplify the problem. A comparison between the near-field and far-field generated distributions is performed, based on a number of evaluation metrics. A method to check for the correctness of the LID from the near-field measurement is discussed. Finally, some possible solutions to eliminate the dynamic range mismatch induced errors are proposed.

2. Equipment

2.1 Near-field goniophotometers

Two out of three near-field goniophotometers (RiGO801-300 and RiGO801-Leuchten, manufactured by TechnoTeam Bildverarbeitung GmbH [13]), which are installed in a darkened room with controlled temperature of (25 ± 1) °C at the Light & Lighting Laboratory of KU Leuven, were used for the measurements described in this study. These two devices are capable of measuring the LID of luminaires of up to 30 cm and 2 m diameter, respectively. Both devices are equipped with three detectors; besides the ILMD and the photometer, a fiber input coupled to a spectroradiometer provides the ability to characterize the DUT spectrally in the far-field.

Within a specified sensing scale, determined from the direction of maximum flux in order to avoid saturation during the scanning process, both devices' photometer (Czibula & Grundmann GmbH) has a dynamic range of 18 bits (S/N ratio of 108 dB). In contrast, for a specified integration time, the dynamic range of both devices' digital camera ILMD (LMK 98-4 by Technoteam) is only 12 bits (S/N ratio of 72 dB).

2.2 Devices under test

The first practical test luminaire, which will further be denoted as DUT 1, consists of a light emitting diode (LED) (Seoul Semiconductors, type N42182, power dissipation P_d = 3.2 W, typical forward voltage V_f = 3.25 V, maximum forward current I_f = 800 mA, typical luminous flux ϕ = 66 lm, 3000 K) on which a white ceramic reflector (CerFlex International) has been installed. A picture of DUT 1 is presented in Fig. 1. The dimensions are 31 mm diameter x 11 mm height.

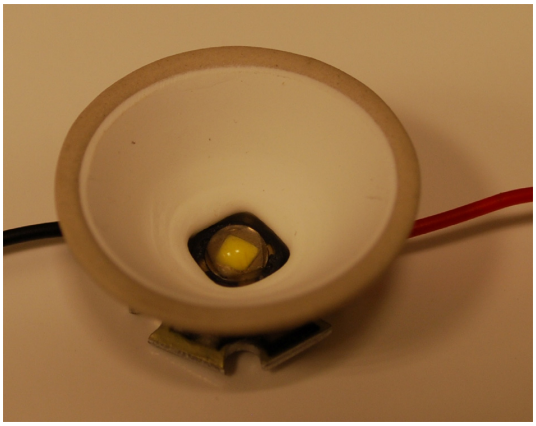

Fig. 1. Picture of DUT 1: an LED with white ceramic reflector.

The second practical example, which will further be denoted as DUT 2, consists of a commercial luminaire (type Duell wall exterior IP44 LED 450lm warm white GI black gold), from the Belgian lighting manufacturer Modular Lighting Instruments [14]. A picture of the luminaire is presented in Fig. 2. The luminaire includes 2 warm-white high power LEDs

#221751 - $15.00 USD Received 26 Aug 2014; revised 10 Dec 2014; accepted 21 Jan 2015; published 28 Jan 2015

(Opulent OP-Rebel Star 2 W, 3000 K), incorporated in a double-walled housing. As such, the luminaire creates a wide fan of light, both upwards and downwards. The product dimensions are 152 mm width x 72 mm depth x 160 mm height.

Fig. 2. Picture of DUT 2: Duell wall exterior from Modular Lighting Instruments.

3. Comparison of measured LIDs

3.1 DUT1

The LID of DUT 1 was first measured in the RiGO801-300 near-field goniophotometer, with the photometer and ILMD revolving about the DUT at a distance of 28 cm. DUT 1 was positioned in a base-up position, and for reasons of thermal stability, operated at I_f = 20 mA (V_f = 2.753 V). Both detectors revolved about the DUT within a range of *C*-planes and γ angles as reported in Table 1. The room temperature *T* during measurement was (25.3 ± 0.1) °C.

Table 1. Installed driveway measurement parameters.

Measurement parameter	Range / Value
C-plane	0° - 360°
Δ*C*-plane	1°
γ	0° - 95°
$\Delta\gamma$	1°

A second measurement of the LID was performed within the RiGO801-Leuchten near-field goniophotometer, in which the distance from the DUT, aligned in the center of the system, to the photometer head equals 147 cm. As such, only the photometer detector was used, and the measurement was considered to be performed under far-field conditions. Again DUT 1 was positioned in a base-up position, and operated at I_f = 20 mA and V_f = 2.754 V. The driveway of the photometer revolving about DUT 1 was similar to the previous measurement (see Table 1). The room temperature *T* during measurement was (25.7 ± 0.1) °C.

The three dimensional (3D) representation of the LID, measured with the RiGO801-300 and the RiGO801-Leuchten near-field goniophotometer, is presented in Fig. 3 and Fig. 4, respectively. At first sight, both LIDs seem to correspond. However, a closer look at the intensity values reveals that the maximum intensity reported by the near-field and far-field

#221751 - $15.00 USD Received 26 Aug 2014; revised 10 Dec 2014; accepted 21 Jan 2015; published 28 Jan 2015

measurement is 1.04 cd and 0.95 cd, respectively. This disagreement of about 9.0% cannot be attributed to the difference in total luminous flux ϕ_t, which numbers 2.219 lm and 2.254 lm (i.e., 1.6% difference), for the near-field and the far-field measurement, respectively. Indeed, an equivalent total luminous flux is expected, since for both measurements this quantity is solely determined by integration of the illuminance values registered by the photometer detector.

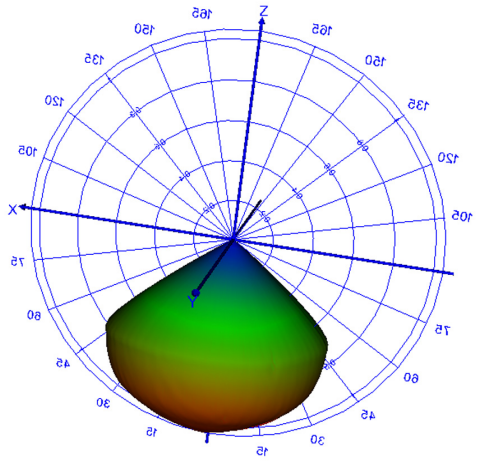

Fig. 3. 3D representation of the LID of DUT 1, measured in the RiGO801-300 near-field goniophotometer (photometer + ILMD detector).

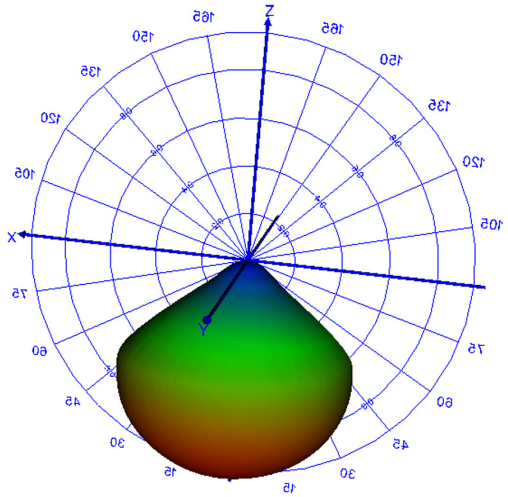

Fig. 4. 3D representation of the LID of DUT 1, measured in the RiGO801-Leuchten near-field goniophotometer (photometer detector).

The significant disagreement between both LIDs can be better visualized by plotting the intensity distributions within one *C*-plane. As an example, the intensity distributions within the 0° *C*-plane ($C0$), obtained from both the near-field (dashed line) and the far-field (solid line) measurement, are presented in Fig. 5.

#221751 - $15.00 USD Received 26 Aug 2014; revised 10 Dec 2014; accepted 21 Jan 2015; published 28 Jan 2015

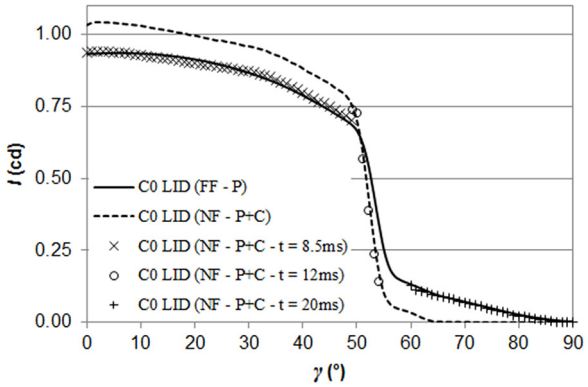

Fig. 5. Comparison between the intensity distributions of DUT 1 in the 0° *C*-plane (*C*0), obtained from the near-field measurement with photometer and camera detector, denoted as '*C*0 LID (NF-P + C)' (dashed line), and the far-field measurement with only a photometer detector, denoted as '*C*0 LID (FF-P)' (solid line). Additionally, the intensity distribution in the 0° *C*-plane, obtained from the combination of 3 near-field measurements over different measurement regions with a different integration time of 8.5 ms, 12 ms, and 20 ms, respectively, is presented (combination of cross points and circles).

The percentage error PE_{LID} between both functions, known as

$$PE_{LID} = 100\left|\frac{I_1(\gamma) - I_2(\gamma)}{I_1(\gamma)}\right| \tag{1}$$

is plotted as a function of γ in Fig. 6. $I_1(\gamma)$ and $I_2(\gamma)$ represent the intensities obtained from the far-field and the near-field measurement at the specified angle γ, respectively. While between γ = 0° and γ = 50° PE_{LID} numbers around 10%, the value increases drastically for larger values of γ. Obviously, a fraction of the flux detected by the photometer at larger γ angles is wrongfully attributed to lower γ angles, due to luminance contributions below the detection limit of the ILMD, which are omitted in the relative luminance distribution images at larger γ angles. This can be made clear by comparing the luminance images acquired with the ILMD with a single exposure time (i.e., the exposure time determined within the near-field measurement), with high dynamic range luminance images obtained by combining acquisitions at different exposure times. As an example, this comparison is presented for two measurement angles in the 0° *C*-plane, i.e., γ = 0° and γ = 70°, in Figs. 7(a)–7(f). Within the single exposure images (Figs. 7(a) and 7(d)), the luminance values of specific regions (e.g. in the proximity of the LED) approximately equal the noise level. From the high dynamic range images obtained by use of multiple exposure times (Figs. 7(b) and 7(e)), on the contrary, it is clear that there is a significant contribution coming from these regions. The difference image, obtained from subtracting the single exposure image from the multiple exposure image, corroborates this finding (see Figs. 7(c) and 7(f)).

#221751 - $15.00 USD Received 26 Aug 2014; revised 10 Dec 2014; accepted 21 Jan 2015; published 28 Jan 2015

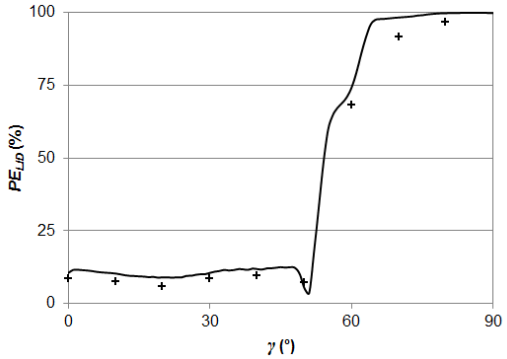

Fig. 6. Percentage error PE_{LID} between the intensity distributions of DUT 1 in the 0° *C*-plane (C0), obtained from the near-field and the far-field measurement, as a function of γ (solid line). Cross points indicate the percentage error, obtained from a sanity check, between illuminance values simulated from ray files and measured, at a photometer distance of 147 cm.

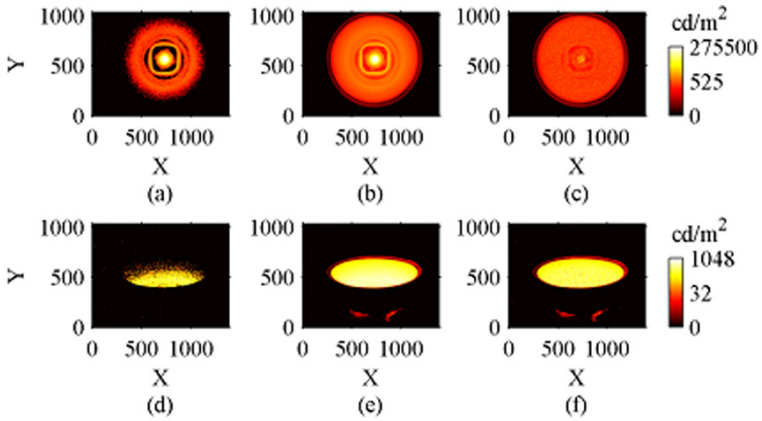

Fig. 7. Comparison of standard dynamic range luminance images of DUT 1, acquired with the ILMD with a single exposure time (left column), with high dynamic range luminance images of DUT 1, obtained from multiple exposures (mid column), at γ = 0° (top row) and γ = 70° (bottom row) in the 0° *C*-plane. Pictures in the right column represent absolute difference images, obtained from subtracting the standard dynamic range image from the high dynamic range image, at the respective γ angle.

For a better comparison of the entire LIDs, a number of metrics have been proposed. Ashdown, for instance, introduced the so-called Hausdorff distance metric, which is however only useful for ranking purposes of several (i.e., more than 2) similar photometric distributions [15].

Bergen proposed the metric $f_{\text{luminaire}}$ for comparison of two LIDs, taking into account and also eliminating discrepancies arising both from misalignment and from differences in luminous flux output [16]. First, the 'goodness of fit' between the two sets of LID data is calculated as:

$$f_{\text{luminaire,fit}} = 100\left(1-\sqrt{\frac{\sum_{C=0}^{360}\sum_{\gamma=0}^{180}\left(I_1(C,\gamma)-I_2(C,\gamma)\right)^2}{\sum_{C=0}^{360}\sum_{\gamma=0}^{180}\left(I_1(C,\gamma)+I_2(C,\gamma)\right)^2}}\right) \tag{2}$$

#221751 - $15.00 USD Received 26 Aug 2014; revised 10 Dec 2014; accepted 21 Jan 2015; published 28 Jan 2015

where $I_1(C,\gamma)$ and $I_2(C,\gamma)$ are the luminous intensities of distributions 1 and 2, respectively, at the angle (C,γ). Afterwards, the optimized value of $f_{\text{luminaire,fit}}$, called $f_{\text{luminaire,max}}$, is determined as the maximum value of $f_{\text{luminaire,fit}}$, by taking into account a scaling factor for the difference in total luminous flux between both distributions ($f_{\text{luminaire,flux}}$), as well as the mounting differences due to rotational and tilt misalignment ($f_{\text{luminaire,spin}}$, and $f_{\text{luminaire,tiltplane}}$ and $f_{\text{luminaire,tiltangle}}$).

While the metric proposed by Bergen makes it possible to compare two LIDs, it still suffers from some inconveniences. First of all, each luminous intensity is equally weighted, i.e., there is a greater weighting given to the data nearby the poles. Second, the correlation between the resulting value of the metric and the degree of agreement between the LIDs seems not straightforward. Indeed, if two LIDs have nothing in common, $f_{\text{luminaire,fit}}$ will equal 0. If, on the other hand, the two LIDs are identical, $f_{\text{luminaire,fit}}$ will equal 100. Yet, according to Bergen, only an $f_{\text{luminaire,fit}}$ value of more than 98 represents a good match [16]. This threshold value seems to have been chosen rather arbitrarily, without any relation to a photometric quantity.

For these reasons, we introduce a new metric, which we call the discrepancy metric *d*, based on the fraction of the total luminous flux that is emitted in a different direction for the two LIDs $I_{1,n}$ and $I_{2,n}$, obtained after normalization of I_1 and I_2 to the total luminous flux ϕ_t:

$$d\left(I_1(C,\gamma), I_2(C,\gamma)\right) = 100\,\frac{\iint_{\gamma\,C}\sqrt{\left(I_{1,n}(C,\gamma)-I_{2,n}(C,\gamma)\right)^2}\,\sin\gamma\,d\gamma\,dC}{2\phi_t} \qquad (3)$$

The two metrics defined in Eq. (2) and Eq. (3), respectively, were calculated for comparison of the presented LIDs. The matching factor $f_{\text{luminaire,fit}}$ numbers 94.07, while the luminous flux scale $f_{\text{luminaire,flux}}$ equals 0.9844. Since $f_{\text{luminaire,flux}}$ is inferior to 1, a scaling of the LID measured under far-field conditions with this factor increases the differences between both LIDs. As such, $f_{\text{luminaire,max}}$ also equals 94.07, meaning that corrections for rotational misalignment and tilt offset do not cancel out the lower matching factor resulting from the scale mismatch correction. Since only an $f_{\text{luminaire,max}}$ value of more than 98 can be considered to be good, the matching result of 94 must be regarded as relatively bad. The calculated discrepancy metric *d* numbers 10.1%, which means that 10.1% of the total luminous flux of the device is emitted in a different direction for the LID generated from the near-field measurement, in comparison to the LID obtained from the far-field measurement.

3.2 DUT2

The LID of DUT 2 was measured twice in the RiGO801-Leuchten near-field goniophotometer; first with both the photometer and ILMD detector, i.e., under near-field measurement conditions, and second with only the photometer detector, i.e., under far-field measurement conditions. The measurements were performed successively, without removing the DUT from the goniometer. In this way, no misalignment errors or tilt shift could occur between the LIDs which are to be compared.

DUT 2 was positioned in a base-up position, and operated at V = 230 V. The other major measurement parameters, together with the reported current I, dissipated power P, and total luminous flux ϕ_t within both measurements, are presented in Table 2. Again, as expected, the total luminous flux of both measurements agrees well.

#221751 - $15.00 USD Received 26 Aug 2014; revised 10 Dec 2014; accepted 21 Jan 2015; published 28 Jan 2015

Table 2. Installed measurement parameters for the LID measurements of DUT 2.

Measurement parameter	Range / Value
C-plane	0° - 360°
ΔC-plane	1°
γ	0° - 173°
$\Delta\gamma$	1°
$T_{\text{near-field}}$	(25.6 ± 0.1) °C
$T_{\text{far-field}}$	(25.3 ± 0.1) °C
$I_{\text{near-field}}$	65.1 mA
$I_{\text{far-field}}$	65.3 mA
$P_{\text{near-field}}$	6.354 W
$P_{\text{far-field}}$	6.364 W
$\phi_{\text{, near-field}}$	130.8 lm
$\phi_{\text{, far-field}}$	130.7 lm

A 3D representation of the LID, measured under near-field and under far-field conditions, is presented in Fig. 8 and Fig. 9, respectively. While for DUT 1 at first sight the LIDs seemed to correspond, a clear difference can now be observed. Besides the two lobes which obviously represent the fan of light as described earlier (see Fig. 2), the LID obtained from the far-field measurement contains 4 smaller lobes, which are absent in the LID generated from the near-field measurement. The contributions within these directions are resulting from specular reflection of the light emitted by the LEDs towards the reflector. Clearly, the ILMD does not detect these contributions because of a too low signal. Remark that also for the other detection angles a significant disagreement between both LIDs is observed, with percentage errors ranging between 5% and 25% in the detection area comprising the two main lobes. This is made clear in Fig. 10, in which the percentage error PE_{LID} between the two distributions in the 0° C-plane is plotted as a function of γ.

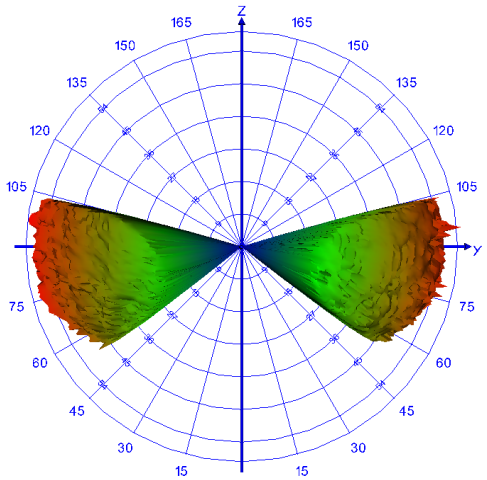

Fig. 8. 3D representation of the LID of DUT 2, measured in the RiGO801-Leuchten near-field goniophotometer (photometer + ILMD detector).

#221751 - $15.00 USD Received 26 Aug 2014; revised 10 Dec 2014; accepted 21 Jan 2015; published 28 Jan 2015

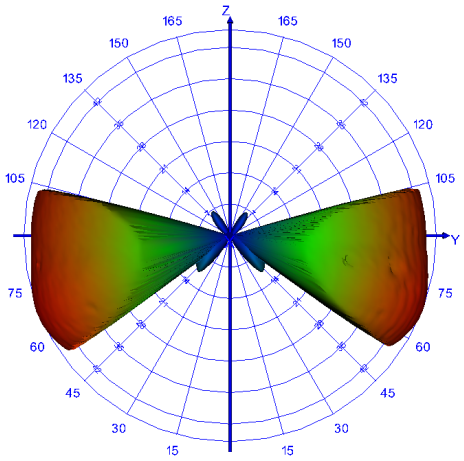

Fig. 9. 3D representation of the LID of DUT 2, measured in the RiGO801-Leuchten near-field goniophotometer (photometer detector).

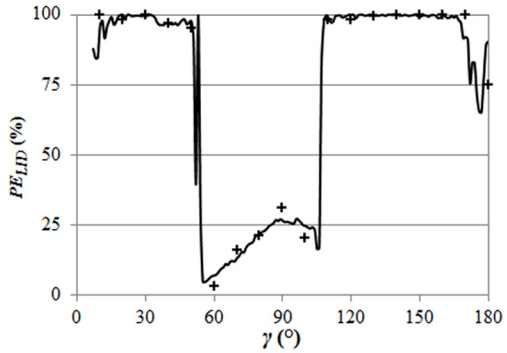

Fig. 10. Percentage error PE_{LID} between the intensity distributions of DUT 2 in the 0° *C*-plane (*C*0), obtained from the near-field and the far-field measurement, as a function of γ (solid line). Cross points indicate the percentage error, obtained from a sanity check, between illuminance values simulated from ray files and measured, at a photometer distance of 147 cm.

Similar as to DUT 1, the two metrics for evaluation of the agreement between the LIDs were calculated for DUT 2. The matching factor $f_{\text{luminaire,fit}}$ numbers 87.27 while the luminous flux scale $f_{\text{luminaire,flux}}$ is equal to 1.0008. After correction, $f_{\text{luminaire,max}}$ equals 87.29. As expected, due to the absence of the 4 smaller lobes in the near-field generated LID, this value is lower than $f_{\text{luminaire,max}}$ of DUT 1, which was 94. The percent amount of the total luminous flux d which is emitted in a wrong direction in the LID generated from the near-field measurement, calculated according to Eq. (3), is now 16.2%.

4. Discussion

In the previous section, it was demonstrated that the dynamic range mismatch between the ILMD and the photometer detector, which are used simultaneously in NFG, may result in the generation of erroneous LIDs. At this moment, no standard way to check for these dynamic range mismatch induced errors is implemented in the commercial proprietary software steering the measurement process of the near-field goniophotometer [17]. However, a so-called sanity check could be incorporated to detect erroneous results. This technique, which was first suggested by Ashdown [18], but which – as far as we know - has never been performed in practice, basically consists of comparing an illuminance value measured with a

#221751 - $15.00 USD Received 26 Aug 2014; revised 10 Dec 2014; accepted 21 Jan 2015; published 28 Jan 2015

photometer at a certain position, to an illuminance value simulated from the generated ray file in the same position. The simulated illuminance value can be calculated by performing a ray intersection algorithm with a surface which has the same size, position and orientation as the photometer [12]. A significant difference between the measured and simulated illuminance would indicate a dynamic range mismatch induced error.

By way of example, this procedure was applied to both DUT 1 and DUT 2. In Fig. 6 and Fig. 10, respectively, the percentage error between simulated and measured illuminance values at a photometer distance of 147 cm (the distance between the DUT and the photometer detector in the RiGO801-Leuchten near-field goniophotometer), is shown for different values of angle γ (cross points). As can be observed, in both cases a good correspondence with the percentage error values found between the near-field and far-field generated LID is obtained.

While with the sanity check it is possible to detect if the LID generated from the near-field measurement is wrong, it is not possible to eliminate or to correct the errors. For that, other solutions could be proposed. For example, as has been demonstrated for DUT 1 (cf. Figs. 7(a)–7(f)), multiple scans could be performed with different integration times set to the ILMD, or by use of multiple neutral density (ND) filters mounted on the ILMD. By analysis of each set of relative luminance images captured in a single direction, saturated pixels could be detected and swapped with non-saturated pixels corrected with a factor to take into account the different integration times or transmittance of the ND filter, respectively. However, this solution has the practical drawback that the measurement would become more time consuming, and multiple scans would result in an increased amount of measurement data. Yet, to demonstrate the usefulness of this solution, a variant of the technique was applied to DUT 1. Three near-field measurements, with a different integration time of 8.5 ms, 12 ms, and 20 ms, respectively, set to the ILMD, were performed over three distinct measurement regions (from $\gamma = 0°$ to $\gamma = 50°$, between $\gamma = 50°$ and $\gamma = 55°$, and beyond $\gamma = 55°$, respectively), and combined afterwards. The intensity distribution in the 0° *C*-plane, resulting from the combined near-field measurements, is presented in Fig. 5 (cross points and circles). Obviously, a much better correspondence to the far-field intensity distribution is obtained than with the original near-field measurement.

A second option, not affecting the measurement time, would be to combine the signal of several pixels into one, i.e., an effective increase of the dynamic range of the camera. Theoretically, a binning of 64x64 pixels would increase the S/N ratio of the ILMD with 36 dB. This effectively closes the gap between the S/N ratio of the ILMD and the photometer, and as a result eliminates the dynamic range mismatch induced errors. However, such a binning decreases the original resolution of the ILMD (1390x1040 pixels) to a resolution of merely 21x16 pixels. While this binning method has been discussed in the literature [18], it has not been performed on such an extreme scale. As such, the influence on the angular and spatial resolution still needs to be investigated.

5. Conclusion

In this paper, two practical examples were presented to demonstrate that the dynamic range mismatch between the ILMD and the photometer detector of a near-field goniophotometer may engender erroneous LIDs and ray files. Although the potential for these errors has been reported before, it is – to the best of our knowledge – the first time that this proposition has been corroborated and quantified in practice. While in the first practical example errors were caused by the fact that luminance values below the detection limit of the ILMD were not incorporated within relative luminance distribution images, in the second example the ILMD mainly did not capture any luminance distribution within specific directions because of a too low signal. By use of the discrepancy metric *d*, which we introduced as an alternative metric to compare LIDs, significant deviations from the actual LID were recorded for both DUTs, with more than 10% and 16% of the total luminous flux being emitted in an erroneous direction.

A method to check for the correctness of the near-field generated LID, the so-called sanity check, was discussed. The described procedure was applied to the two DUTs. In both cases, a

#221751 - $15.00 USD Received 26 Aug 2014; revised 10 Dec 2014; accepted 21 Jan 2015; published 28 Jan 2015

good agreement with the percentage error values found between the near-field and far-field generated LID was obtained, corroborating the applicability of the method.

Finally, some possible solutions to eliminate the errors arising from the dynamic range mismatch were discussed. These included the application of several scans with different exposure times set to the ILMD, and the combination of the signal from multiple adjacent pixels into one. A variant of the former alternative, in which several scans performed with different integration times over different measurement regions are stitched, was applied to DUT 1. It was demonstrated that the resulting near-field LID obviously better corresponds with the far-field LID than in the original measurements. This result suggests that applying this method in sequential runs with different integration times over the entire hemisphere, i.e., a universal application of high-dynamic range images, could resolve the errors induced by the dynamic range mismatch. Future research may focus on simulating the effectiveness of these alternatives with virtual experiments by use of a computer model [9], in order to further quantify their impact and effectiveness over the current working method.

Acknowledgments

The authors wish to thank the Hercules Foundation for the financial support regarding the near-field goniophotometer equipment under grant AKUL-35.

#221751 - $15.00 USD Received 26 Aug 2014; revised 10 Dec 2014; accepted 21 Jan 2015; published 28 Jan 2015